Applications of graphene in nanotechnology : 1D diffusion, current drag and nanoelectrodes

Vrbica, S.

A

APPENDIX
DIFFUSION OF CO ADATOMS

A1. 1D RANDOM WALK PROBABILITY DISTRIBUTION FOR CO ON GNR

We assume that an atom makes only nearest-neighbor jumps between sites arranged along a line, and motion to the right or to the left is equally probable and occurs at random moments in time. The probability P of an atom, initially at position $x = 0$ at time $t = 0$ to be at lattice site x at time t is given by [1]

$$P_x(\nu) = Ae^{-2\nu t} I_x(2\nu t) \tag{A.1}$$

where A is the prefactor, ν is the hopping rate and I_x modified Bessel function of the first order

$$I_x(a) = \sum_{i=0}^{\infty} \frac{1}{i!(i+k)!}\left(\frac{a}{2}\right)^{2i+x}. \tag{A.2}$$

As time t we take the average duration of the voltage pulse (0.5 sec).

[1] J. D. Wrigley *et al.*, Lattice walks by long jumps, J. Chem. Phys. 93, 2885 (1990)

A

A2. 2D RANDOM WALK PROBABILITY DISTRIBUTION FOR CO ON AU

The top image in Figure A.1 shows hollow sites on Au(111) which are presumably preferential spots for Co adatoms. The black dot in the center indicates the initial Co position (no displacement), red dots indicate 2nd- nearest-neighbor displacement, brown dots indicate 4th- nearest-neighbor displacement and so on. The two nearest hollow sites are 1.7 Å apart, which is at the limit of our resolution. In order to simplify the description, we remove half of the hollow lattice sites (small white circles) and introduce two non-orthogonal axes (bottom image). Each hollow site corresponds to a displacement d and is labeled with a pair of indices, (x,y). Colors indicate category of displacement d and shade indicates different distances from the initial position (black dot in the center) for a given d.

For the two-dimensional random walk on a triangular grid the average number of image-to-image diffusion steps for each of the two dimensions is $\nu t/2$, where ν is the total hopping rate for all four directions. The probability distribution for finding the adsorbate displaced in each of the directions by x and y lattice sites is given by[2]

$$P_{xy} = e^{-\bar{N}} I_x\left(\frac{\bar{N}}{2}\right) I_y\left(\frac{\bar{N}}{2}\right) = e^{-\nu t} I_x\left(\frac{\nu t}{2}\right) I_y\left(\frac{\nu t}{2}\right) \tag{A.3}$$

where I_x, I_y are modified Bessel functions of the first order. We calculate the probability for each L as the sum of all probabilities of the displacements d (none, 1st nearest-neighbor, 2nd nearest-neighbor...) of that length L. For example, the expected probability for Co to be displaced by 0.6 nm is equal to

$$\begin{aligned} P_{L=0.6}(\nu) &= P_{1,-1} + P_{-1,1} + P_{0,2} + P_{0,-2} + P_{2,0} + P_{-2,0} + \\ &+ P_{1,2} + P_{2,1} + P_{-2,-1} + P_{-1,-2} + P_{2,2} + P_{-2,-2} = \\ &= e^{-\nu t}\left[2 I_{\frac{1}{2}} I_{\frac{1}{2}} + 4 I_0 I_1 + 4 I_{\frac{1}{2}} I_1 + 2 I_1 I_1\right] \end{aligned} \tag{A.4}$$

This is also illustrated in the table in the lower panel of Figure A.1. As mentioned in subsection 2.8.3, each L corresponds to a 0.3 nm wide set of values (e.g. L = 0.6 nm takes all values from 0.45 to 0.75 nm). Because of the freely chosen range of data sets, some histogram peaks might be significantly higher/lower than the neighboring ones due to encompassing more/less data points. This explains the sudden drop of the fitted value of probability in Figure 2.28 at 1.2 nm.

[2] J. D. Wrigley *et al.*, Lattice walks by long jumps, J. Chem. Phys. 93, 2885 (1990)

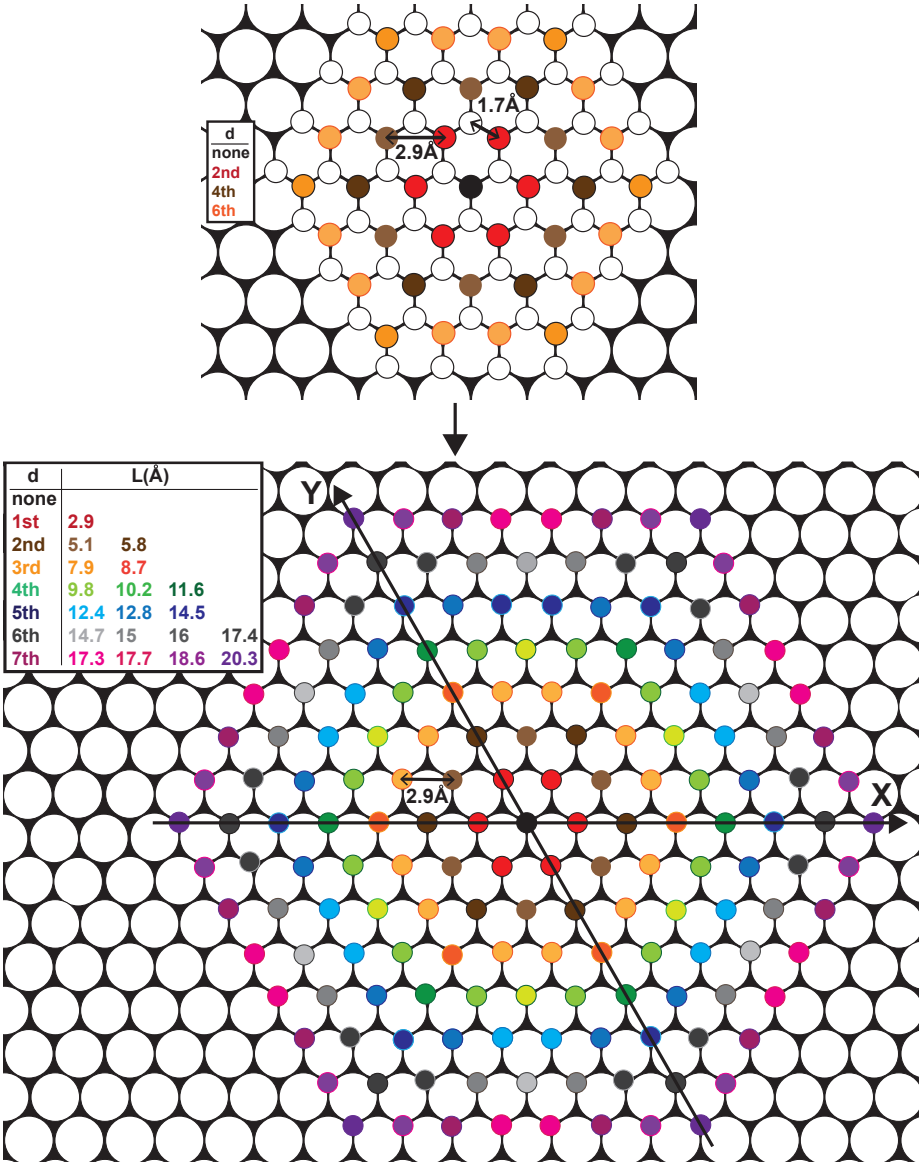

Figure A.1: **Possible displacements for Co on Au(111)**. Top image shows available hollow sites (small circles) which form a hexagonal lattice. The colors indicate the displacement d (none, 1^{st}, 2^{nd}...) from the initial position (black circle in the middle). Small white circles indicate sites that cannot be resolved with our resolution. After removing these sites a trigonal lattice is obtained (bottom image). Different color shades indicate different distances from the initial site (black circle) for the same displacement number. The black dot in the center indicates the initial Co position.

B

APPENDIX
GRAPHENE ELECTRODES

B1. SIMMONS MODEL FOR SYMMETRIC BARRIER

Considering tunneling through a symmetric barrier, we can approximate the work function ϕ to be the same for both electrodes. The current density in a symmetric tunnel junction with a barrier along the z-axis (Figure B.1) is described by the Simmons model [1]:

$$J \sim \frac{e}{2\pi h z^2}\left[(\phi-\mu_L)e^{\frac{-4\pi z\sqrt{2m(\phi-\mu_L)}}{h}} - (\phi-\mu_R)e^{\frac{-4\pi z\sqrt{2m(\phi-\mu_R)}}{h}}\right] \tag{B.1}$$

where $z = z_1 - z_2$ is the gap size, and μ_L, μ_R are the chemical potentials of the left and the right electrodes, respectively.

Parameters fitted to the Simmons model are the pre-factor A (which contains the cross-section of the junction), the barrier height ϕ and the gap size z. The parameters A and ϕ cannot be fitted completely independently, but with a suitable choice for the pre-factor the barrier height obtained is in agreement with the range of results found in the literature, see the main text. The gap distance d is more robust and it is estimated with approximately 5% accuracy.

[1] J. G. Simmons. Generalized formula for the electric tunnel effect between similar electrodes separated by a thin insulating film. *J. Appl. Phys.*, 34: 1793-1803, 1963.

B

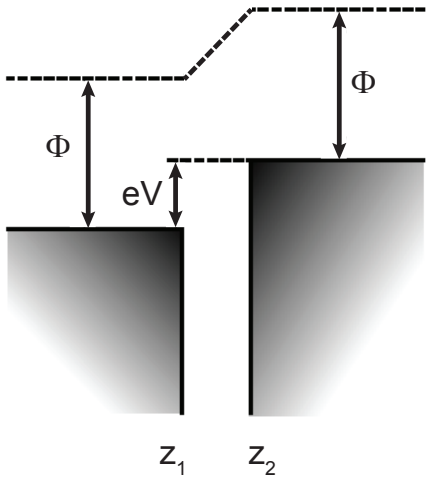

Figure B.1: **Symmetric tunnel junction with barrier height ϕ and barrier width d = $z_1 - z_2$.**

B2. GRAPHENE-GOLD TUNNEL JUNCTION

In order to identify the edge electrodes that extend to the end of their supports, we formed a tunneling junction against a gold sample. This, in first instance, allows easier electrical characterization of the edge electrode and secondly demonstrates the flexibility of our system, capable of employing independent edge electrodes in multiple systems, either symmetric or asymmetric junctions.

Figure B.2(a) illustrates the schematics of the set-up. The graphene edge electrode is mounted on a holder over a piezoelectric actuator (thick grey block on the left) which approaches a thick sample of pure gold. Figure B.2(b) shows the I(V) tunneling characteristic of the tunnel junction at a fixed distance, sweeping the bias voltage V between -1.5 V and + 1.5 V. The shape of the sigmoidal IV curve is characteristic of an asymmetric tunneling barrier. This is a result of the different work functions across the two terminals of the junction. Figure B.2(c) shows the tunneling current as a function of distance (black curve, I(z)) between the graphene and the gold sample at V = 0.48 V bias voltage. We observe a clear exponential increase (exponential fit red curve) of the current with decreased distance, characteristic of a tunneling regime.

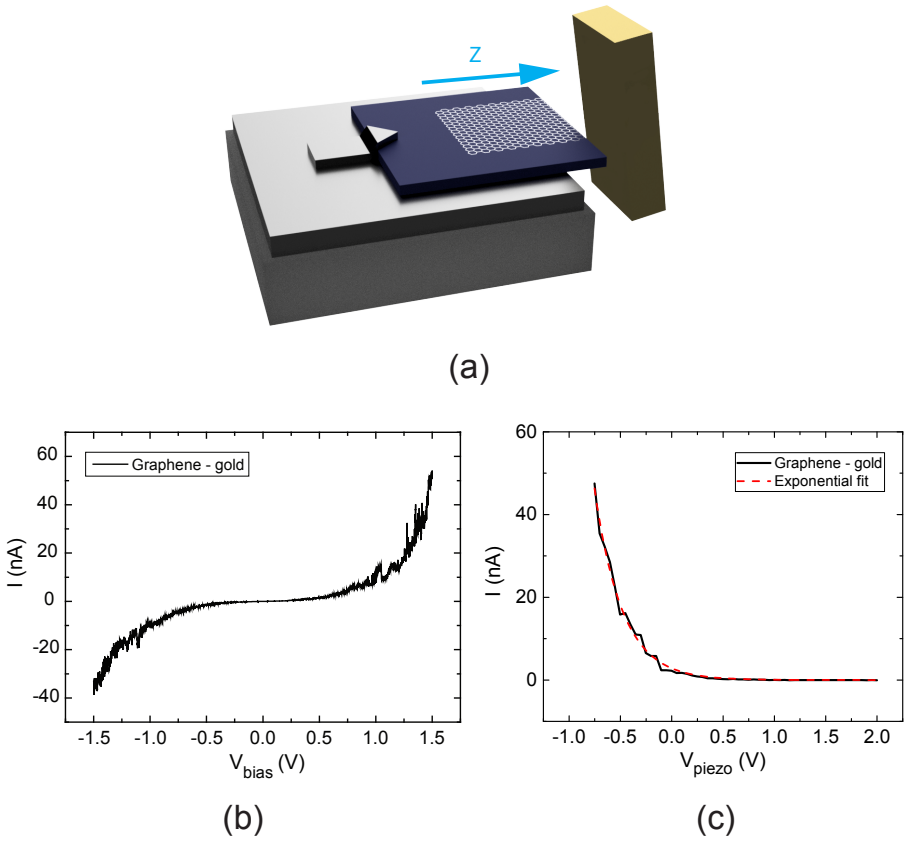

Figure B.2: **Gold-graphene tunnel junction.** (**a**) Schematics of the gold – graphene tunnel junction. The graphene electrode is mounted on a piezoelectric actuator which moves the sample along the Z axis to approach a gold macro electrode. (**b**) IV characteristic of the graphene-gold junction. (**c**) Representative I(z) characteristic of graphene-gold tunnel junction (black line) fitted to exponential function (red line).

B3. TUNNELING JUNCTION CONTROLLER

The two graphene sheets are mounted on sample stages at the positions of "sample" and "tip" of an STM scanner. A description of the scanner can be found in PhD dissertation of S. Otte [2]. Graphene was contacted electrically by a drop of silver paint embedding a copper wire attached to the sample stage. A RHK SPM-100 controller was used to supply bias voltage between the samples, as well as the high voltage for Z piezo element that is moving one of the supports. The tunneling current flowing across the junction was amplified using a FEMTO DLPCA-200 current amplifier. The XY motion was controlled by a second piezo element underneath the other support. The voltage applied to the XY piezo element was kept constant during I(z) and IV measurements.

B4. SHEET RESISTANCE AND POINT CONTACT RESISTANCE

In contrast to 3D metallic systems the point contact resistance measured here has a large contribution from the sheet resistance of the graphene electrodes that cannot be separated from the measurements. The total measured resistance is the quantum point contact resistance, R_{pc}, in series with the classical resistance of the sheets, R_g. The classical resistance R_g of the sheets on either side of the contact can be estimated as

$$R_g = \frac{1}{\pi\sigma}\int_{l_0}^{L}\frac{1}{r}dr \tag{B.2}$$

where σ is the sheet conductance, L is the size of the graphene sample (2 mm), and l_0 is the electron mean free path. Using the semi-classical expression for the sheet conductance:

$$\sigma = \frac{e^2}{h}\frac{2E_F\tau}{\hbar} \tag{B.3}$$

and the linear dispersion of the Fermi energy $E_f = \hbar v_F k_F$, and $k_F = \sqrt{\pi n}$, we can express the mean free path in terms of the conductivity and the electron density:

$$l_0 = \frac{\sigma}{\frac{e^2}{h}}\frac{1}{2\sqrt{\pi n}} \tag{B.4}$$

Using the conductance of $\sigma = (11 \pm 2)\frac{e^2}{h}$ found for our samples, and the typical dependence between charge density and conductance in this regime [3,4] we obtain an estimate of $l_0 = 27$ nm. With this we arrive at an estimated resistance for the sum of the two graphene electrodes of 17 ± 3 kΩ. Subtracting this value from the measured

[2] S. Otte. Magnetism of a single atom. *PhD thesis*, 2008

[3] K. S. Novoselov, A. K. Geim, S. V. Morozov, D. Jiang, M. I. Katsnelson, I. V. Grigorieva, S. V. Dubonos, A. A. Firsov. Two-Dimensional gas of massless Dirac fermions in graphene. *Nature*, 438: 197-200, 2005

[4] E. H. Hwang, S. Adam, S. Das Sarma. Carrier transport in two-dimensional graphene Layers. *Phys. Rev. Lett.*, 98:186806, 2007.

point contact resistance of 28 kΩ, we find an estimate for the quantum point contact resistance of:

$$R_{\text{qpc}} = R_{\text{total}} - R_{2\text{g}} = 11 \pm 3k\Omega \tag{B.5}$$